JOURNAL OF GEOPHYSICAL RESEARCH, VOL. 100, NO. C1, PAGES 773–778, JANUARY 15, 1995

A note on the bimodal directional spreading of fetch-limited wind waves

I.R. Young and L.A. Verhagen

Department of Civil Engineering, University College, University of New South Wales, Canberra, Australia

M.L. Banner

School of Mathematics, University of New South Wales, Sydney Australia

Abstract. Measurements of the directional spectra of fetch-limited wind waves are presented. The directional spreading functions for these spectra are unimodal and narrowest in the region of the spectral peak frequency. Consistent with previous measurements, the spreading broadens for frequencies just above and below the spectral peak frequency. At frequencies of approximately twice the peak frequency, however, the unimodal spreading becomes bimodal, and more wave energy propagates at an angle to the wind than in the wind direction. The bimodal sidelobes continue to separate with increasing frequency and become larger in magnitude. Results obtained with a numerical model with a full solution to the nonlinear terms indicate that the bimodal structure is maintained by directional transfer of energy through nonlinear wave-wave interactions.

1. Introduction

As a result of a large number of field experiments, a detailed empirical understanding of the development of the one-dimensional frequency spectrum has developed [e.g., *Hasselmann et al.*, 1973; *Donelan et al.*, 1985]. The observed structure of the spectrum has been viewed as the result of a balance between the processes of atmospheric input, "whitecap" dissipation, and nonlinear interactions [e.g., *Hasselmann et al.*, 1973; *Komen et al.*, 1984; *Banner and Young,* 1994]. The directional spectrum is, however, less well understood. The inclusion of directionality places significantly higher demands on observational systems, which in turn has limited the number of available data. In addition, the inclusion of directionality places more stringent demands on models. As a result, both the experimental database and theoretical explanations for observed directional spreading are incomplete.

It is the purpose of this note to present preliminary data from a high-resolution spatial array. The design of the array is such that it is possible to obtain reliable directional data to frequencies as high as 3 times the spectral peak ($3f_p$) and possibly higher. At these higher frequencies, previously unseen structure is apparent in the directional spreading function. These findings are consistent with results from calculations using a state-of-the-art wind wave prediction model that shows that the observed directional spreading is controlled largely by nonlinear interactions within the spectrum.

Paper number 94JC02218.
0148-0227/95/94JC-02218$05.00

2. Previous Observations of Directional Spreading

There are three commonly quoted sources for data on the directional spreading of wind generated waves: the data of *Mitsuyasu et al.* [1975], *Hasselmann et al.* [1980] and *Donelan et al.* [1985]. *Mitsuyasu et al.* [1975] and *Hasselmann et al.* [1980] both used pitch-roll buoy systems to obtain their data. In contrast, *Donelan et al.* [1985] utilized a spatial array with a large number of wave gauges (14). Recently, *Young* [1994] has examined the directional resolving power of these respective instruments, showing that the spatial array, not surprisingly, has significantly higher resolving power. Consequently, pitch-roll buoys yield directional spreading broader than that obtained using a higher-resolution instrument. The differences between these data sets can be explained in this manner, with the pitch-roll buoy results of *Mitsuyasu et al.* [1975] and *Hasselmann et al.* [1980] yielding directional spreading broader than that reported by *Donelan et al.* [1985]. Qualitatively, however, the trends observed in these various data are consistent. Directional spreading functions are monotonic, with most energy propagating in the wind direction, and decay with increasing angle to the wind. *Mitsuyasu et al.* [1975] and *Hasselmann et al.* [1980] represented this dependence in the form $\cos^{2n}(\theta/2)$, whereas *Donelan et al.* [1985] adopted $\mathrm{sech}^2\beta\theta$, where θ is the angle to the mean wind direction and n and β are frequency-dependent parameters which determine the rate of decay of wave energy with increasing θ.

All data sets show that the directional spreading is narrowest in the region of the spectral peak f_p and broadens at frequencies both higher and lower than f_p.

The pitch-roll buoy data extend to frequencies as high as $3f_p$, but the directional resolving power of these instruments decreases with increasing frequency [*Young,* 1994]. The higher-resolution data of *Donelan et al.* [1985] extend only to $1.6f_p$.

The functional dependence of the parametric representations developed from these data sets also vary. Both *Mitsuyasu et al.* [1975] and *Hasselmann et al.* [1980] indicate the directional spreading is a function of both the nondimensional frequency f/f_p and the inverse wave age U_{10}/C_p, where U_{10} is the wind speed measured at a reference height of 10 m and C_p is the phase speed of the spectral peak frequency. In contrast, *Donelan et al.* [1985] could detect no dependence on the inverse wave age, with their directional spreading dependent only on f/f_p. *Donelan et al.* [1985] argue that this is an indication that nonlinear interactions play the dominant role in determining the directional spreading with atmospheric input providing only a secondary contribution.

3. Measured Directional Data

As part of a larger wave dynamics experiment [*Young and Verhagen,* 1993], measurements of the directional wave spectrum have been made in Lake George, Australia. Data was obtained with a spatial array consisting of seven gauges as shown in Figure 1. The gauges were arranged in the form of a "Mercedes star" with a central gauge and two rings of three gauges at radii of 0.20 m and 0.55 m. The resolving power of this type of instrument has been investigated by *Young* [1994]. The gauges were coincidently burst sampled at 8 Hz and the

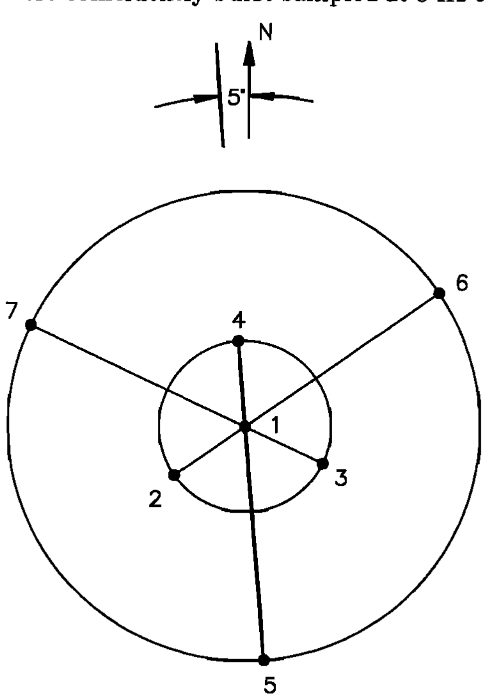

Figure 1. Configuration of the seven-element spatial array used in Lake George. The gauges in the inner circle are at a radius of 0.20 m, and those in the outer circle are at a radius of 0.55 m.

directional spectrum formed using the maximum likelihood method (MLM) [*Isobe et al.,* 1984; *Young,* 1994].

Lake George is approximately 20 km long by 10 km wide with the long axis aligned north-south. The effects of slanting fetches and lake geometry can be seen in many of the directional spectra (not shown here). To overcome these complicating effects, only data for which the wind direction was approximately normal to the long north-south shorelines are considered in this note (i.e., easterly or westerly winds). As the wind is normal to a long and approximately straight shoreline, these data sets closely approximate the ideal case of fetch-limited growth. In addition, only cases for which the wind speed varied by less than 10% and the wind direction by less than 10° over the 30-min data collection period were considered.

The directional frequency spectrum $E(f,\theta)$ is commonly represented in terms of the one-dimensional frequency spectrum $F(f) = \int E(f,\theta)d\theta$ through the use of the directional spreading function $G(f,\theta)$,

$$E(f,\theta) = N(f)G(f,\theta)F(f) \tag{1}$$

where $N(f)$ is a normalization function, and in the present definition we assume that $G(f)$ has a maximum value of unity at each frequency.

Figure 2 shows six examples of the directional spreading function G obtained with the instrumentation described earlier. Each panel shows G at nondimensional frequencies f/f_p equal to 1, 2, and 3. In each case the wind direction is shown by the vertical solid line. The cases shown have inverse wave ages U_{10}/C_p ranging between 1.7 and 3.0. Four of the cases are for westerly winds, and two are for easterly winds. All the examples shown in Figure 2 have similar features. As was reported in previous data, the spectrum is narrowest in the region of the spectral peak, with the peak energy closely aligned with the wind direction. Consistent with these previous measurements, the spectrum broadens with increasing frequency. Rather than remaining unimodal, however, it develops a bimodal structure with sidelobes approximately symmetrically placed around the mean wind direction. The slight asymmetry is believed to be due to statistical sampling variability. The magnitude of these sidelobes and the angle from the wind direction at which they are located both increase with increasing frequency. A clearer representation of the directional spreading is shown in Plate 1. Plates 1a and 1b show shaded contour plots of the spreading functions as functions of f/f_p and θ for the two spectra previously shown in Figures 2c and 2e, respectively (i.e., a westerly and an easterly case). In this figure it is clear that the spreading is narrowest and unimodal in the region of the spectral peak. At frequencies less than the spectral peak the spreading increases significantly but remains unimodal. At frequencies greater than the spectral peak the spreading gradually increases. The unimodal structure exhibited at the spectral peak becomes flat-topped by $f/f_p = 1.7$ and bimodal by $f/f_p = 2.0$. The sidelobes continue

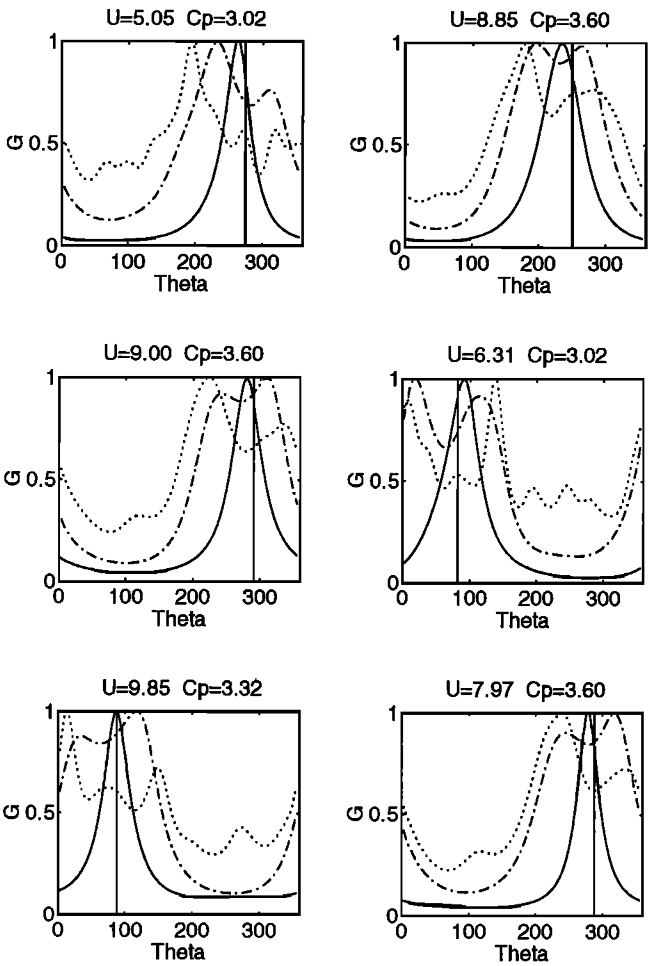

Figure 2. Examples of the directional spreading function G as a function of direction. Spreading functions are shown at $f/f_p = 1$ (solid line), $f/f_p = 2$ (dash-dot line) and $f/f_p = 3$ (dotted line). The horizontal axis shows direction in the "coming from" convention. The wind speed and phase speed at the spectral peak frequency are shown at the top of each panel. The vertical solid line corresponds to the wind direction.

to separate in direction with increasing frequency. At $f/f_p = 4.0$, the approximate high-frequency limit of the array, the lobes are separated by almost 180° (90° from the wind direction).

The "noise floor" in the spectra obtained with the maximum likelihood method is clearly apparent in Figure 2. This level clearly rises with increasing frequency, but the signal to noise ratio is still high at $f/f_p = 3$ and reasonable at $f/f_p = 4$ (see Plate 1). It is not possible to resolve higher frequencies, as the finite spacing between the gauges leads to spatial aliasing. Extensive testing with simulated analytical forms for the input time series were used to ensure that the observed bimodal structure was not an artifact of the analysis technique. In addition, repeated analysis of the data progressively reducing the number of gauges consistently reproduced the bimodal structure. Naturally, as the number of gauges is reduced, the directional resolving power of the array is reduced, eventually becoming so degraded as to mask the presence of the sidelobes.

Similar semianalytical tests by *Tsanis and Brissette* [1992] and *Young* [1994] for a variety of directional spreading widths show that the MLM reproduces the actual spreading with reasonable accuracy. It has a tendency to artificially broaden the spectrum but does not produce spurious peaks where none exist in reality. Hence we conclude that the bimodal structures reported here are not an artifact of the analysis technique.

4. Comparison With Previous Data Sets

If the bimodal directional structures reported above are a consistent feature of fetch limited waves, one must address the question of why they are not apparent in the directional data sets discussed in section 2. The pitch-roll buoy data of both *Mitsuyasu et al.* [1975] and *Hasselmann et al.* [1980] were analyzed using a model specific technique, direct Fourier expansion [*Longuet-Higgins et al.,* 1963]. This technique explicitly assumes a unimodal spreading function of the form $\cos^{2n}\theta/2$, hence excluding the possibility of the bimodal forms reported here.

In contrast, the model-independent analysis of *Donelan et al.* [1985] and the high directional resolution of their spatial array should be capable of reproducing the forms reported here. The data of *Donelan et al.* [1985], however, extend only to $f/f_p = 1.6$. At such frequencies, the present data indicate directional spreading that is still unimodal, the bimodal structure becoming apparent only above $f/f_p = 2$. Figure 3 shows a comparison of the directional spreading functions for the two cases shown in Plate 1 with the $\mathrm{sech}^2\beta\theta$ parameterizations of *Donelan et al.* [1985]. For each spectrum, comparisons are made at $f/f_p = 1.0$ and 1.5. The present results are comparable with those of *Donelan et al.* [1985], although they appear to be marginally broader.

There are a number of published data sets which provide some support for the bimodal features reported here. *Holthuijsen* [1983] used airborne stereophotography to measure the directional spectrum of waves in the North Sea. Although less clearly defined than in the present results, his spectra show bimodal spreading. Jähne and Riemer [1990] used an imaging optical technique to determine the directional spectra of laboratory waves. Their directional wavenumber spectra clearly show bimodal spectra at wavenumbers above the spectral peak. *Brissette and Wu* [1992] used a three-element array to measure directional spectra in Lake St. Clair, Canada. They used a normalized MLM [*Brissette and Tsanis,* 1992] to analyze their data, obtaining results similar to those reported here. Unable to explain the observed bimodal spreading, they speculated that it was a result of refraction by currents.

5. Physical Processes Controlling Directional Spreading

Hasselmann [1963a, b] and *Hasselmann et al.* [1973] have clearly demonstrated that nonlinear interactions

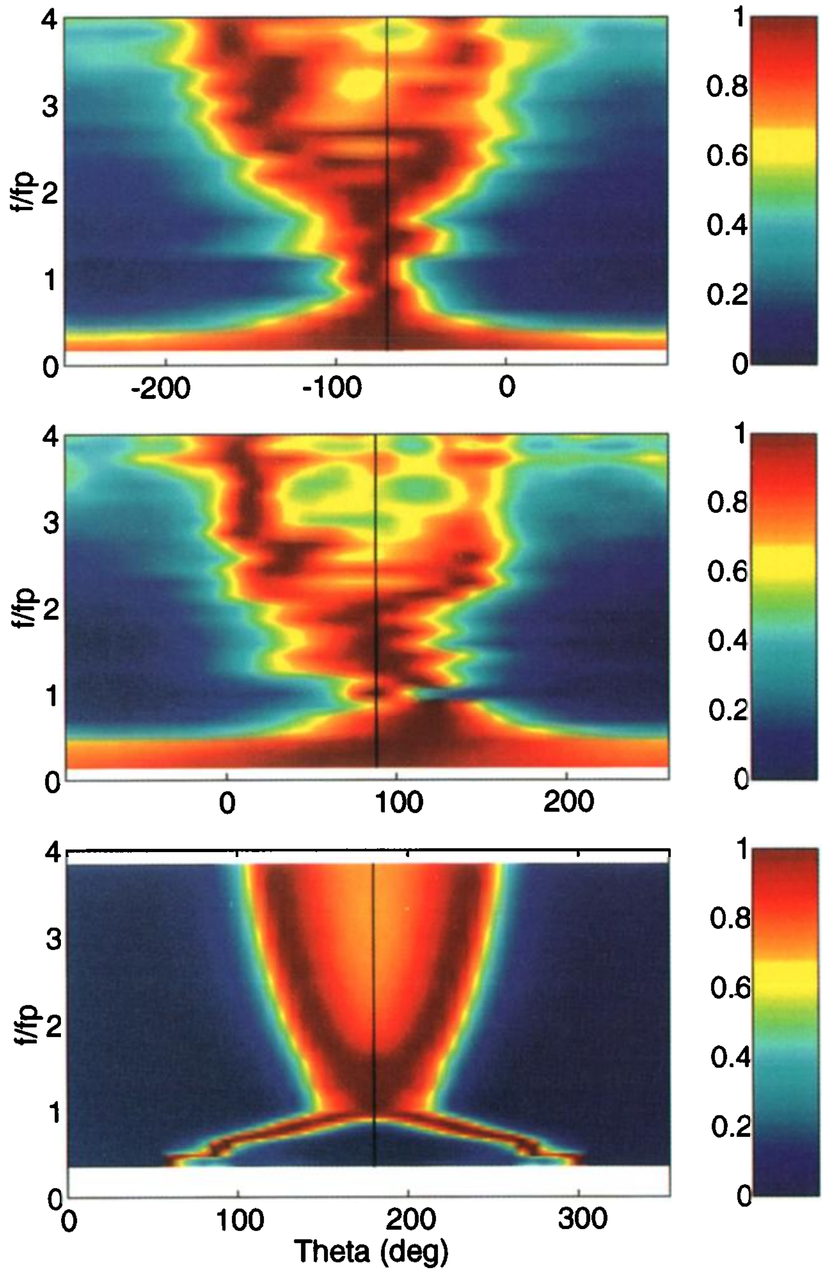

Plate 1. Color shaded images of the directional spreading function G as a function of direction and nondimensional frequency f/f_p, corresponding to the functions shown in (a) Figures 2c and (b) Figure 2e. Panel (c) shows the results of the fetch-limited spectral model with a full solution to the non-linear terms. The inverse wave age for the numerical result in Plate 1c is $U_{10}/Cp \approx 3$ and is approximately the same as the measured data in Plates 1a and b. The direction axes for all panels have been rotated so that the mean propagation direction is centrally located on the plot.

play a dominant role in the evolution of the one-dimensional spectrum, and *Donelan et al.* [1985] have speculated that they are also dominant in determining the directional spreading. The existence of the bimodal directional structures reported above requires elucidating the processes which could give rise to these forms. *Young and Van Vledder* [1993] and *Banner and Young* [1994] have reported results from a numerical model that includes a full solution to the nonlinear source term. The model is very similar to that used by *Komen et al.* [1984] except that it removes assumptions about the explicit form of the high-frequency tail shape. A typical example of the directional spreading function obtained with this model is shown in Plate 1c. Although there are differences in detail, the qualitative features produced by the model are consistent with the results reported here. In particular, the model produces directional spreading functions that are unimodal at $f/f_p = 1$ but bimodal at higher frequencies. As was shown by *Banner and Young* [1994], the precise

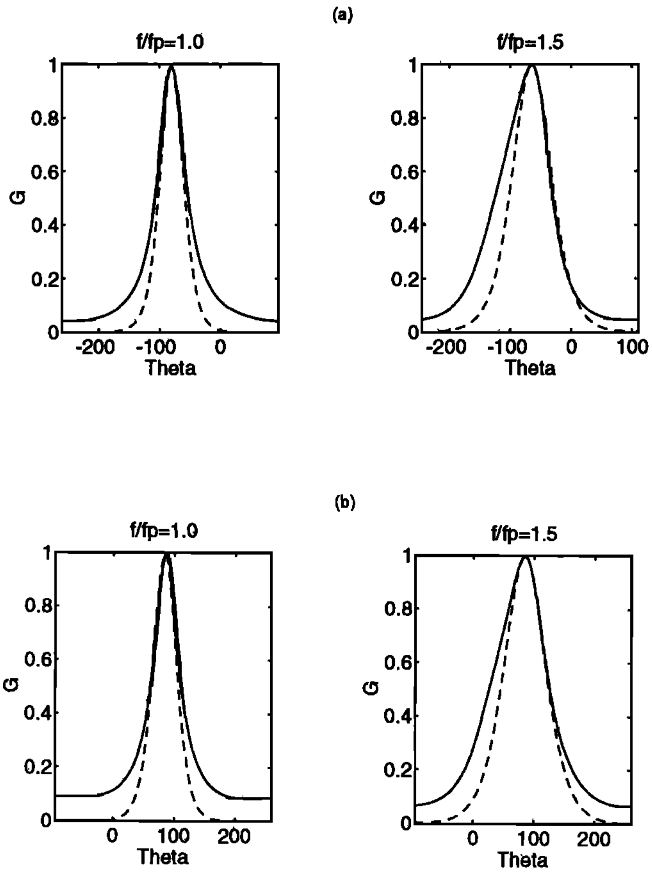

Figure 3. Comparisons of the measured directional spreading functions G (solid line) with the parametric form proposed by *Donelan et al.* [1985] (dashed line), corresponding to spectra shown in (a) Plate 1a and (b) Plate 1b. Comparisons are made at $f/f_p = 1.0$ and 1.5. The direction axis has been rotated so that the mean propagation direction is centrally located on the plot.

magnitude of the sidelobes varies with the choice of the source terms for atmospheric input and dissipation in the model. Their existence is, however, a robust feature of the model and is controlled by the nonlinear term. One of the properties of the nonlinear term is the transfer of energy from the mean wind direction to angles to the wind, thus yielding the bimodal spreading.

The model also yields very strong bimodal spreading for $f/f_p < 1$, in contrast to the measured results, which are broad and unimodal in this region. The reason for these differences is not clear, but it is interesting to speculate on possible causes. The atmospheric input adopted in the model is that of *Komen et al.* [1984], which assumes no energy input to spectral components propagating faster than the wind or to components with zero initial energy (i.e., a purely exponential growth mechanism). Both the measured spectra and the numerical result shown in Plate 1 are for quite young wind seas, $U_{10}/C_p \approx 3$. Hence spectral components at frequencies immediately below the peak will propagate significantly slower than the wind speed. Therefore, provided such components have nonzero energy, there will be a positive input from the wind. Although the spectra of the measured data decrease in magnitude very rapidly for frequencies less than the spectral peak, there is always a small but finite residual energy present. The model spectra, however, have zero initial energy at these frequencies. Hence there is no atmospheric input in the model at frequencies below the peak, the bimodal spreading being controlled by the nonlinear terms. The small but finite atmospheric input at these frequencies for the field data appears to be sufficient to dominate the nonlinear terms and form a unimodal directional distribution at frequencies less than the spectral peak.

6. Conclusions

This short note has provided the first detailed evidence for the existence of bimodal directional spreading functions for wind generated waves. The results are consistent with the directional data of *Donelan et al.* [1985] in the region of validity of these data (i.e., $f/f_p < 1.6$), showing unimodal spreading in this range. At approximately $f/f_p = 2$ the spreading function develops into a bimodal form with more energy at an angle to the wind than in the wind direction. The existence of these bimodal directional forms is supported by the model results of *Young and Van Vledder* [1993] and *Banner and Young* [1994], who have shown that the spreading in this region is controlled by the nonlinear spectral transfer term.

The full implications of such spreading functions are difficult to assess, but it is reasonable to assume that any of the microwave instruments that image the high-frequency region of the spectrum will be sensitive to the exact form of the directional spreading. As the bimodal structure develops beyond $f/f_p = 2$, where the spectral energy is small compared to the region closer to the peak, it is probable that the existence of the bimodal spreading will have little impact for engineering applications.

The existence of the bimodal spreading does, however, provide additional support for the validity of the *Hasselmann* [1962] type four-wave weak nonlinear interaction theory that is able to predict the existence of such forms.

Acknowledgments. The experimental program through which the data presented in this note was obtained was supported financially by the Australian Research Council. This assistance is gratefully acknowledged. The original version of the computer model used to perform the calculations presented in Plate 1c was provided by Donald Resio of the Florida Institute of Technology. His assistance is appreciated.

References

Banner, M.L., and I.R. Young, Modelling spectral dissipation in the evolution of wind waves, 1, Assessment of existing model performance, *J. Phys. Oceanogr.*, *24*, 1550-1671, 1994.

Brissette, F.P., and I.K. Tsanis, Maximum likelihood method techniques for directional analysis of heave-pitch-roll data, paper presented at Third International Workshop on Wind Hindcasting and Foreasting, Environment Canada, Montreal, Canada, 1992.

Brissette, F.P., and J. Wu, Wave directional spectra and current interaction in Lake St. Clair, paper presented at Third International Workshop on Wind Hindcasting and Foreasting, Environment Canada, Montreal, Canada, 1992.

Donelan, M.A., J. Hamilton, and W.H. Hui, Directional spectra of wind-generated waves, *Philos. Trans. R. Soc. London, A, 315*, 509-562, 1985.

Hasselmann, D.E., M. Dunckel, and J.A. Ewing, Directional wave spectra observed during JONSWAP 1973, *J. Phys. Oceanogr., 10*, 1264-1280, 1980.

Hasselmann, K., On the non-linear energy transfer in a gravity-wave spectrum, 1, General theory, *J. Fluid Mech., 12*, 481-500, 1962.

Hasselmann, K., On the non-linear energy transfer in a gravity-wave spectrum, 2, Conservation theorems; wave-particle analogy; irreversibility, *J. Fluid Mech., 15*, 273-281, 1963a.

Hasselmann, K., On the non-linear energy transfer in a gravity-wave spectrum, 3, Evaluation of energy flux and swell-sea interaction for a Neumann spectrum, *J. Fluid Mech., 15*, 385-398, 1963b.

Hasselmann, K., et al., Measurements of wind-wave growth and swell decay during the Joint North Sea Wave Project (JONSWAP), *Dtsch. Hydrogr. Z., 8*, (12), suppl. A, 95pp., 1973.

Holthuijsen, L.H., Observations of the directional distribution of ocean-wave energy in fetch-limited conditions, *J. Phys. Oceanogr., 13*, 191-207, 1983.

Isobe, M., K. Kondo, and K. Horikawa, Extension of MLM for estimating directional wave spectrum, paper presented at Symposium on Description and Modelling of Directional Seas, DHI and MMI, Copenhagen, 1984.

Jähne B., and K.S. Riemer, Two-dimensional wave number spectra of small-scale water surface waves, *J. Geophys. Res., 95*, 11,531-11,546, 1990.

Komen, G.J., S. Hasselmann, and K. Hasselmann, On the existence of a fully developed wind-sea spectrum, *J. Phys. Oceanogr., 14*, 1271-1285, 1984.

Longuet-Higgins, M.S., D.E. Cartwright, and N.D. Smith, Observations of the directional spectrum of sea waves using the motions of a floating buoy, in *Ocean wave spectra*, Prentice Hall, Englewood Cliffs, N.J., pp.111-136, 1963.

Mitsuyasu, H., F. Tasai, T. Suhara, S. Mizuno, M. Ohkuso, T. Honda, and K. Rikiishi Observations of the directional spectrum of ocean waves using a cloverleaf buoy, *J. Phys. Oceanogr., 5*, 750-760, 1975.

Tsanis I.K., and F.P. Brissette, Methods for directional spectra measurements by small arrays, paper presented at Third International Workshop on Wind Hindcasting and Foreasting, Environment Canada, Montreal, Canada, 1992.

Young, I.R., On the measurement of directional wave spectra, *Appl. Ocean Res.*, Elsevier, (in press), 1994.

Young, I.R., and G.Ph. Van Vledder, A review of the central role of nonlinear interactions in wind-wave evolution, *Philos. Trans. Roy. Soc., London, A, 342*, 505-524, 1993.

Young, I.R., and Verhagen, L.A., The evolution of wind-waves in finite depth water, in *The Air-Sea Interface*, edited by M.A. Donelan, W.H. Hui, and W.J. Plant, University of Toronto Press, Toronto, 1993.

I.R. Young and L.A. Verhagen, Department of Civil Engineering, University College, University of NSW, Northcott Drive, Canberra, ACT 2600, Australia. (e-mail: iry@waves.ce.adfa.oz.au)

M.L. Banner, School of Mathematics, University of NSW, Sydney, NSW 2052, Australia

(Received January 14, 1994; revised May 6, 1994; accepted August 1, 1994.)